Eur Biophys J (2010) 39:1433–1444
DOI 10.1007/s00249-010-0599-6

ORIGINAL PAPER

Understanding the role of thiol and disulfide self-assembled DNA receptor monolayers for biosensing applications

Laura G. Carrascosa · Lidia Martínez · Yves Huttel · Elisa Román · Laura M. Lechuga

Received: 2 October 2009 / Revised: 27 January 2010 / Accepted: 3 March 2010 / Published online: 1 April 2010

Abstract A detailed study of the immobilization of three differently sulfur-modified DNA receptors for biosensing applications is presented. The three receptors are *DNA-(CH)n-SH-*, *DNA-(CH)n-SS-(CH)n-DNA*, and *DNA-(CH)n-SS-DMTO*. Nanomechanical and surface plasmon resonance biosensors and fluorescence and radiolabelling techniques were used for the experimental evaluation. The results highlight the critical role of sulfur linker type in DNA self-assembly, affecting the kinetic adsorption and spatial distribution of DNA chains within the monolayer and the extent of chemisorption and physisorption. A spacer (mercaptohexanol, MCH) is used to evaluate the relative efficiencies of chemisorption of the three receptors by analysing the extent to which MCH can remove physisorbed molecules from each type of monolayer. It is demonstrated that –SH derivatization is the most suitable for biosensing purposes as it results in densely packed monolayers with the lowest ratio of physisorbed probes.

L. G. Carrascosa · L. M. Lechuga
Grupo de Nanobiosensores y Aplicaciones Bioanalíticas (nanoB2A), CIBER de Bioingeniería, Biomateriales y Nanomedicina (CIBER-BBN), 08193 Bellaterra, Barcelona, Spain

L. G. Carrascosa (✉) · L. M. Lechuga
Grupo de Nanobiosensores y Aplicaciones Bioanalíticas (nanoB2A), Centro de Investigación en Nanociencia y Nanotecnología (CIN2) CSIC-ICN, 08193 Bellaterra, Barcelona, Spain
e-mail: lcarrascosa@cin2.es

L. Martínez · Y. Huttel · E. Román
Instituto de Ciencia de Materiales de Madrid (ICMM-CSIC), Cantoblanco, Madrid 28049, Spain

Keywords Thiolated DNA · Biofunctionalization · Surface plasmon resonance biosensor · Nanomechanical biosensor · Fluorescence · XPS

Introduction

DNA evaluation is crucial in diverse areas of molecular biology. Besides standard methods of detection, biosensor devices are an interesting alternative tool because they can rapidly detect DNA hybridization in real-time and label-free. Most state-of-the-art biosensing methods use gold-ended transducers and biofunctionalization is carried out by self-assembly of thiol-derivatized DNA receptor molecules on the sensing surface.

There is extensive knowledge of how different thiol-derivatized molecules self-assemble on to gold surfaces, especially for alkanethiols. For alkanethiols, either thiol or disulfide-derivatized, dense monolayers can be obtained (Bain et al. 1989; Jung et al. 1998; Biebuyck et al. 1994; Wackerbarth et al. 2004; Fenter et al. 1994; Garg et al. 2000; Noh and Hara 2001; Noh et al. 2000). In dialkyl disulfides, cleavage of the S–S bond rapidly occurs at room temperature after adsorption on the gold surface, because of a dissociative adsorption mechanism that leads to identical alkanethiolate species as the alkanethiols (Noh and Hara 2001). However, once adsorption is complete, it is unclear whether or not the final quality of the self-assembled monolayers (SAMs) derived from alkanethiols and dialkyl disulfides are identical. As an example, SAMs derived from alkanethiols and the equivalent dialkyl disulfide are indistinguishable when examined by ellipsometry or X-ray photoelectron spectroscopy (XPS) (Bain et al. 1989; Biebuyck et al. 1994), whereas the use of other in-situ methods, for example second harmonic generation

(SHG, also called frequency doubling) (Jung et al. 1998) or thiol-thiol exchange measurements (Bain et al. 1989), found disulfides which chemisorb 40% slower than alkenothiols; furthermore, chemisorption of thiols is favoured compared with disulfides (75:1). These results suggest that the higher steric hindrance of disulfides could be a key issue which differentiates the quality of the disulfide monolayers from their alkanethiol counterparts. The discrepancy between different methods to analyse the self-assembly process could be attributed to the physical property monitored in the analysis. Techniques that are sensitive to the formation of the sulfur–gold bond, for example second harmonic generation (SHG), are able to detect the differences between both types of monolayer, contrary to those unable to distinguish between physisorbed and chemisorbed states.

When working with biological receptors such as DNA, the intrinsic properties of DNA, for example its polyanionic structure or its conformational properties, add more complexity to the evaluation of their behaviour during immobilization. Unlike alkanethiol self-assembly, which only involves covalent attachment of the headgroup (linker) and interchain van der Waals interactions, the assembly process for sulfur modified DNA molecules includes linker–surface contributions, lateral interactions among neighbouring DNA chains, and nonspecific strand–surface interactions via nucleotide–gold contacts. Although nonspecific interactions significantly participate in the immobilization of DNA and directly affect the kinetics, orientation, and surface coverage during the self-assembly process (Wolf et al. 2004), no systematic investigation has been carried out to evaluate the effect of the thiol linker type used for DNA assembly over these interactions.

On the other hand, thiolated tethered probes are quickly oxidized to disulfide species if no reduction treatment is carried out. This is a spontaneous dimerization reaction which occurs even when the DNA solution is kept at very low temperatures. Because of this, most companies do not offer DNA in the SH form but, instead, provide a disulfide version, for example DNA-SS-DMTO. This molecule has the DNA chain coupled through the disulfide bridge to a short molecule (dimethoxytrityl, DMTO), which stabilizes the DNA-SH molecule. This type of DNA can be used for immobilization in the disulfide form; the DMTO group can, however, also be removed before the immobilization in order to furnish pure DNA-SH.

Chemical reduction of disulfides from the sample is a tedious, time-consuming, and reagent-consuming task. But if DNA thiols and disulfides behave similarly during self-assembly, starting from the thiol-derivatized or the disulfide version, chemical reduction would be irrelevant.

Therefore, it is of special interest to establish whether there is a dependence on linker type during self-assembly and if this affects the extent of physisorption. Physisorption should be avoided as much as possible in order to obtain a maximized and reproducible specific biosensing response. In addition, for DNA testing, it is also relevant to understand how the linker type affects the crowding, conformation, and orientation of immobilized DNA, factors which could affect the final hybridization efficiency.

We have carried out a detailed study of the immobilization of three differently sulfur-modified DNA molecules, using a short alkanethiol, 1-β-mercaptohexanol (MCH). MCH reduces DNA physisorption phenomena when it is added after DNA adsorption. This molecule displaces the non-specific adsorptive contacts between nucleotides and gold and occupies the vacant places within the monolayer (Herne and Tarlov 1997). It is used to quantify the extent of chemi/physisorption for a given DNA SAM, merely by analysis of this displacement effect.

For this study, we selected:

1 a DNA thiol form, DNA–$(CH)_6$–SH;
2 the corresponding symmetric ssDNA disulfide form, DNA–$(CH)_6$–SS–$(CH)_6$–DNA; and
3 an asymmetric ssDNA disulfide form in which the disulfide group bridges the same DNA molecule with a dimethoxytrityl group (DMTO), DNA–$(CH)_6$–SS–DMTO.

Use of the two different disulfide forms enabled us to analyse the effect of the molecules linked at both sides of the sulfur bridge (long and charged DNA chain in the case of the symmetric disulfide; small and uncharged DMTO chain in the case of the asymmetric disulfide) on the self-assembly process.

In previous work we have evaluated the self-assembly and the effect of MCH adsorption on these three DNA monolayers by using XPS (Martínez et al. 2010). Here, we evaluated:

1 the DNA immobilization efficiency in chemisorption;
2 the time-dependence of DNA self-assembly; and
3 the organization and spatial configuration on the three DNA monolayers before and after MCH adsorption

By use of XPS, two biosensor devices (a surface plasmon resonance sensor and a nanomechanical biosensor), and fluorescence and radiolabelling techniques.

Biosensor devices enable real-time monitoring of DNA immobilization and MCH adsorption. Surface plasmon resonance (SPR) sensing is a widespread technique for the detection of a broad variety of analytes (Homola 2008). Nanomechanical biosensors provide a sensitive way of analysing the adsorption of biomolecules on solid surfaces, and is also sensitive to structural changes of the adsorbed biological molecules (Moulin et al. 2000) which could help to differentiate between chemisorbed and physisorbed states during DNA self-assembly.

Fluorescence is an useful method for characterization of DNA monolayers, giving information about the spatial–conformational distribution of DNA molecules within the monolayer (Stoermer and Keating 2006; Rant et al. 2004a, b; Arinaga et al. 2006; Lee et al. 2006). This technique exploits the inter-distance (d)-dependent quenching effect between gold and fluorophores, by following a $1/d^5$ behaviour (Chance et al. 1978). Finally, radiolabelling enables quantification of the adsorbed probes regardless the type of adsorption, because this method cannot differentiate between chemisorbed and physisorbed probes.

Combination of the results from all detection methods could provide a comprehensive view of the process of immobilization of DNA, paying special attention to the role of the type of thiol linker.

Experimental

Samples

DNA samples were single-stranded oligonucleotides, 12-mer long (5′-AACGACGGCCAG-3′), purchased from Genomechanix, LLC (USA) and functionalized with different sulfur modification at the 5′ or 3′ end as follows:

i. thiol linker: SH–$(CH_2)_6$–5′-DNA-3′ (hereafter called DNA-SH)
ii. dimethoxytrityl-disulfide linker: DMTO–SS–$(CH_2)_6$–5′-DNA-3′ (hereafter called DNA-SS-DMTO)
iii. disulfide linker: 5′-DNA-3′–$(CH_2)_6$–S–S–$(CH_2)_6$–3′-DNA-5′ (hereafter called DNA-SS-DNA)

A unmodified form of DNA was used as negative control.

Substrates

For the SPR measurements we used cover glass slide (10 mm × 10 mm × 0.15 mm) coated with 2 nm titanium and 45 nm gold, (SSens, The Netherlands). For XPS, similar substrates were used, but fabricated by e-beam evaporation. For the nanomechanical sensor, we used commercial silicon nitride cantilevers (Veeco Instruments, USA), 200 μm long, 40 μm wide, 0.6 μm thick, and gold-coated at both sides. The original gold coating was removed in order to obtain surfaces that maximize the surface stress response of the cantilever. Removal of original gold was achieved by rinsing the chip in aqua regia (3:1 HCl–HNO_3); 5 nm chromium and 20 nm gold were then deposited by thermal evaporation at only one of the cantilever sides immediately before the experiments.

For fluorescence and radiolabelling experiments, 25 mm × 75 mm × 1.5 mm microscope slides covered with 2 nm titanium and 45 nm gold (EMF Corporation, USA) were used. Before immobilization, substrates were thoroughly cleaned and sonicated with organic solvents (trichloroethylene, acetone, and ethanol) and distilled water. For the nanomechanical sensors the sonication process was avoided to prevent cantilever damage. To complete the cleaning procedure, the substrates were dipped in a freshly prepared piranha solution (3:1 H_2SO_4–H_2O_2), followed by rinsing and sonication in distilled water and, finally, drying with N_2.

Substrate cleaning and, especially, the piranha procedure were skipped for substrates used for XPS measurements, to prevent sulfur atoms from the sulfuric acid solution contributing to the measured sulfur peak. To preserve the gold surface from any external contamination, immobilization procedures were performed immediately after gold deposition.

Immobilization and MCH post-treatment

Immobilization procedures were carried out using a 1 μM concentration of the oligo sample prepared in a buffered solution (50 mM sodium phosphate–1 M NaCl) for a short time (5 min) and/or overnight (15 h). The two selected immobilization times enabled analysis of the organization and the spatial configuration of the oligonucleotides, and study of physi/chemisorption processes, in the initial stage of immobilization (short immobilization time) and when all possible reorganization effects had taken place (overnight). Therefore, monolayer changes, such as reorganizations and variation of the surface densities or chemi/physisorption ratios, as a consequence of the immobilization time, could be detected.

For XPS, fluorescence, radiolabelling, and SPR biosensor techniques, DNA immobilization was done ex-situ. For SPR and XPS, the solution was gently dropped until the gold surface of the chip was fully covered, whereas for fluorescence and radiolabelling experiments, 1 μL droplets were deposited on the gold slides. After immobilization, samples were rinsed with deoinized water and dried under a nitrogen flow. For the nanomechanical biosensor, immobilization was done in flux inside the fluid cell using the same conditions as in the ex-situ procedure.

For the biosensors, MCH post-treatment was done in flux, whereas for fluorescence and XPS techniques were carried out ex-situ, by gently dropping 1 mM MCH solution in buffer (50 mM sodium phosphate–1 M NaCl) on the previously immobilized monolayers for 5 min.

Surface plasmon resonance biosensor

A commercial surface plasmon resonance biosensor, from Sensia (Spain), was used. The sensor has two flow cells,

each with a volume of 300 nL. The device incorporates optics, upgradeable electronic modules, and computer-controlled pumps, valves, and injection fluidics. All the measurements were done by injection of the sample using the flow-delivery system, which ensures the injection of precise volumes of 220 μL while maintaining a continuous flow of buffer between 10 and 40 μL/min. Further description of this system can be found elsewhere (Mauriz et al. 2006).

Nanomechanical biosensors device

Experiments were carried out using a home made device, including a single microcantilever with optical read-out, using a static detection scheme. This detection method relies on changes of the cantilever surface stress due to the adsorption of molecules on to the microcantilever surface. Further description of this system can be found elsewhere (Alvarez et al. 2004).

Fluorescence and radiolabelling methods

For fluorescence measurements, the oligonucleotides are CY3-fluorescent labelled at the 3′ end which is the opposite extreme of the thiol linker structure. The fluorescence was detected with a confocal fluorescent scanner (Scan Array 4000, GSI Lumonics).

For radiolabelling experiments, the oligonucleotides were also labelled at the 3′ end using ^{32}P. The signal of ^{32}P labelling was detected by autoradiography and use of a Geiger counter.

XPS

XPS measurements were performed in an ultra high-vacuum (UHV) chamber with a base pressure of 1×10^{-10} mbar. The angle between the hemispherical analyser (Specs-PHOIBOS100) and the surface plane was kept at 60° and the X-ray radiation employed was the Mg K_α line (1253.6 eV). The survey spectra were recorded with a photon energy step of 0.25 eV and a pass energy of 40 eV, whereas the S 2p and Au 4f core levels were measured with a photon energy step of 0.1 eV and a pass energy of 15 eV. In order to increase the signal-to-noise ratio of the S 2p core level spectra, multiple scans were accumulated for each sample. Analysis of the individual scans (acquired in groups of 150 accumulated scans) was performed in order to ensure the stability of each system studied in UHV. Before the data analysis, the contributions of the MgK_α satellite lines were subtracted and the spectra were subjected to linear background subtraction formalism. The binding energy (BE) scale was calibrated relative to the Au 4f7/2 peak at 83.8 eV. Fittings were carried out using Gaussian–Lorentzian (GL) doublets with a standard spin–orbit splitting of 1.2 eV, a S 2p1/2/S 2p3/2 branching ratio of 1:2[16,17,18] and the same full width at half maximum (FWHM) (1.3 ± 0.1 eV).

The method used for calculation of the S coverage and further description of XPS experiments can be found elsewhere (Martínez et al. 2010).

Results and discussion

Study of DNA immobilization and DNA chemisorption efficiency

Immobilization of the three types of DNA was explored by use of nanomechanical sensors and radiolabelling. All three sulfur-modified ssDNA molecules caused significant bending of the cantilever of hundreds of nanometers (Fig. 1a). Mean values (σ) of 210 ± 60, 110 ± 20 and 70 ± 30 mN/m were found for DNA-SH, DNA-SS-DMTO, and DNA-SS-DNA, respectively (Fig. 1b).

An unmodified DNA molecule was also evaluated to obtain a reference for physisorption, because this molecule does not bear any sulfur modification able to be attached to the gold surface. The unmodified DNA gave a value of 25 ± 15 mN/m, a much smaller surface stress signal than any of the sulfur-modified ones (Fig. 1b). The difference in responses for both modified and unmodified DNA molecules could be explained by either:

a) The presence of the sulfur modification leads to a larger number of molecules at the cantilever surface compared with the unmodified-DNA case. This difference in the loaded mass affects the surface stress resulting in greater cantilever bending.
b) The amount of loaded molecules is similar in both cases regardless of the modification status. However, the difference in the surface stress signals is caused by the different adsorption mechanism (chemisorption vs physisorption).

To properly interpret the nanomechanical results, it is worth mentioning that for this sensor there are two working modes: static and dynamic. The dynamic mode is the only one sensitive to changes in mass loading while the static one, (the mode used in our experiments), is only sensitive to changes in the surface stress at the cantilever surfaces. Determination of the origin of the surface stress response is not straightforward and many different phenomena have been described which could bend the cantilever as a result of surface stress (Alvarez et al. 2004). To address the origin of the nanomechanics response during DNA immobilization it is important to use an alternative method, for example radiolabelling, which provides information about

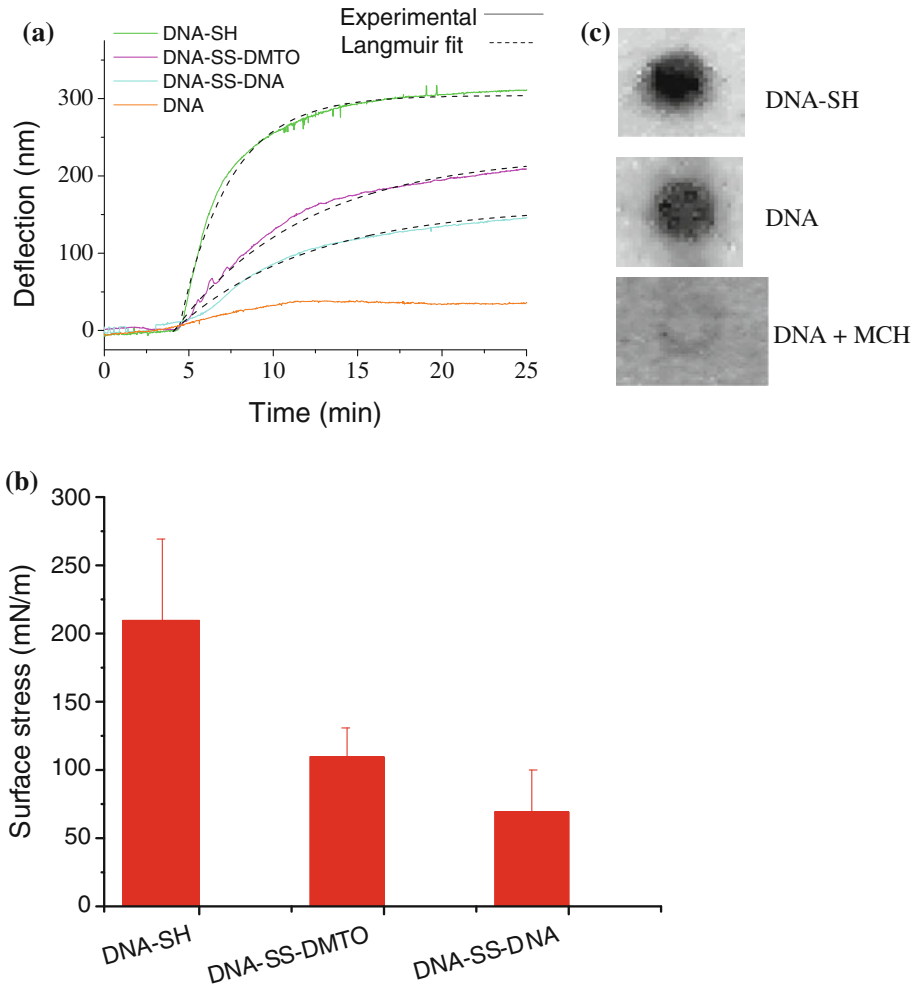

Fig. 1 **a** Nanomechanical deflection curves and fitting to a Langmuir model. **b** Mean surface stress values of DNA immobilization on a nanomechanical biosensor for the three thiol linker types. **c** Radiolabelling images of DNA-SH, the unmodified DNA form and the latter exposed to MCH, which shows the effect of MCH of removing of unbound physisorbed molecules

the surface density irrespective of the adsorption mode (physisorption or chemisorption). We imaged the unmodified DNA and the DNA-SH form by radiolabelling and a similar surface density was found (Fig. 1c). The radiolabelling signal was also measured using a Geiger counter to estimate the surface density. For DNA-SH the surface density was 2.7×10^{12} molecules/cm^2 whereas for the unmodified DNA it was 1.58×10^{12} molecules/cm^2. This latter value confirms the relevance of physisorption phenomena on gold surfaces described in the literature (Wolf et al. 2004). The different DNA loaded mass seems to be insufficient to explain the large difference between their nanomechanical responses because the surface density for DNA-SH was only 1.5 times larger than that for unmodified DNA, whereas the DNA-SH surface stress signal was about eight times larger. These data demonstrate that the surface stress response mainly originates from their different modes of adsorption and that the nanomechanical biosensor is able to differentiate between chemisorbed and physisorbed molecules. According to these findings, we can state that the larger is the cantilever bending, the larger is the amount of chemisorbed probes at the cantilever surface. Therefore the DNA-SH would be the species with the highest ability to chemisorb, compared with the disulfide-modified forms. The DNA-SS-DNA had the lowest ability, giving a deflection signal a factor of three lower than that of the SH form.

We also followed up the temporal evolution of the surface stress during adsorption of the modified oligonucleotides. The behaviour is fitted with a simple Langmuir adsorption isotherm model (Fig. 1a). Good agreement is found between the experimental surface stress curves and the fitting ones. The k values obtained by use of the fitted curves do not represent reaction rate constants but inverse fitted time constants. They only enable following of the temporal evolution of adsorption of the molecules without giving any extra information about the immobilization reaction. Fitted curves suggest that the change in surface stress is proportional to the number of molecules adsorbed on the gold. SH-DNA was the fastest adsorbing molecule with $k = 0.31 \pm 0.06$ min^{-1}, whereas disulfide species were adsorbed more slowly, with very similar adsorption

rate constants: $k = 0.19 \pm 0.05$ and $k = 0.20 \pm 0.04$ min^{-1} for DNA-SS-DMTO and DNA-SS-DNA, respectively.

Kinetic results strongly suggest that the larger values found for the SH form could have their origin in its higher ability to chemisorb, forming dense monolayers more easily than the disulfide forms. This agrees with previous results for alkyl disulfides which found lower adsorption rates for disulfides (Bain et al. 1989).

Effect of the immobilization time on DNA self-assembly

We have studied the effect of immobilization time during DNA self-assembly by use of XPS (Martínez et al. 2010), because on alkanethiol systems the use of long immobilization times for both alkanethiols and dialkyl-disulfides led to the same surface coverage and identical monolayers (Bain et al. 1989; Jung et al. 1998; Biebuyck et al. 1994).

The results, which were discussed in depth in our previous paper (Martínez et al. 2010), are summarised in Table 1. They show that for *short immobilization time* (5 min) the DNA-SH achieved the largest surface density with 9.9×10^{13} molecules/cm^2. Lower surface densities of 5.6×10^{13} and 6.9×10^{13} molecules/cm^2 were found for DNA-SS-DMTO and DNA-SS-DNA, respectively. This means that at the initial stage of immobilization the DNA-SH monolayer was about 1.4 times denser than the DNA-SS-DNA and 1.7 more than the DNA-SS-DMTO. These values were about one order of magnitude larger than those obtained from radiolabelling experiments, probably because of the method used for surface density calculation from the Au/S ratio of the XPS spectra (Martínez et al. 2010). The discrepancy found with the radiolabelling coverages shows that XPS calculations can overestimate the surface coverage. However, they are still valid for comparing the different systems studied in this work, because the overestimation was comparable for all.

When *longer immobilization times* are considered, a surface density increase (2.1×10^{14} molecules/cm^2) was found in the DNA-SH case, whereas for the DNA-disulfides no surface density increase, but a measurable decrease (4.2×10^{13} for DNA-DMTO and 1.8×10^{13} for DNA-SS-DNA) of previously immobilized molecules was observed, which was especially notable for the DNA-SS-DNA case. The increase in the immobilization time led to a DNA-SH monolayer about five times more densely packed than the DNA-SS-DMTO one and eleven times more packed than the DNA-SS-DNA one.

XPS experiments also enabled evaluation of the effect of immobilization time on the ratio of molecules chemisorbed in form of thiolates to physisorbed ones, by analysing the components (S1 and S2) of the deconvoluted XPS spectrum sulfur peak. The proportion of thiolates chemisorbed on the surface can be extracted from the S1 component (Bain et al. 1989; Huang et al. 2005; Cavalleri et al. 2001, 2004; Wirde et al. 1997; Munro and Frank 2003; Sako et al. 2005; Willey et al. 2005; Zerulla et al. 1998; Zhang et al. 2005), whereas the S2 component mainly represents physisorbed species (Wackerbarth et al. 2004; Garg et al. 2000; Cavalleri et al. 2001), although there are some contribution from disulfides (Bain et al. 1989; Cavalleri et al. 2004; Wirde et al. 1997; Zerulla et al. 1998) and, to a limited extent, from the formation of sulfur species because of damage by ionising radiation (Cavalleri et al. 2001; Willey et al. 2005).

Table 1 shows the S1 and S2 values for the three DNA types. DNA-SH and DNA-SS-DNA behaved similarly when considering immobilization in its initial stage. Both displayed about 70–80% of molecules in the chemisorbed state, which was in contrast with the nanomechanical results that showed a much lower proportion of DNA-SS-DNA chemisorbed probes since the beginning of the immobilization. The discrepancy might be caused by the different methodology employed for immobilization, because the nanomechanical experiments are performed in flux. Nevertheless, when considering the XPS results for long immobilization times, both methods agree that DNA-SS-DNA was less able to chemisorb (S1 = 61%) in comparison with DNA-SH (S1 = 80%). This could mean that performing the immobilization in flux led to DNA-monolayers similar to those obtained by ex-situ methods at long immobilization times. In addition, when using longer immobilisation times (1 h or more) in the nanomechanical biosensor, disulfides never achieved the high deflection levels shown by the DNA-SH form (data not shown). This indicates that the monolayers achieved in the nanomechanical biosensor are unable to suffer any further change in their adsorption mode, and therefore physisorbed probes are unable to later chemisorb. A decrease in the deflected signal because of desorption was not observed either.

XPS results showed that, besides the initial ratio of chemisorption of DNA-SS-DNA, this molecule was more unable to chemisorb, displaying high physisorption tendency and even desorption with time. The DNA-SS-DMTO was also less suitable than the DNA-SH form for chemisorption and for the creation of densely packed monolayers. This was in agreement with other results reported in the literature, demonstrating that DNA disulfides have a high percentage of sulfur atoms in a physisorbed state (Wackerbarth et al. 2004).

Desorption found for DNA disulfides, along with their lower ability to chemisorb and to create dense monolayers, could be because of the greater difficulty of proper cleavage of their disulfide bridge and chemisorption in the form of thiolates compared with the dialkyldisulfide case in the

Table 1 Martinez et al. (2010) results of DNA immobilization and MCH treatment analysed by XPS

DNA immobilization								
Species	Short time				Overnight			
	% S	Molecules/cm^2	% S_1 component	% S_2 component	% S	Molecules/cm^2	% S_1 component	% S_2 component
DNA-SH (1)	8	9.9×10^{13}	79	21	18	2.1×10^{14}	81	19
DNA-SS-DMTO (2)	5	5.6×10^{13}	54	46	4	4.2×10^{13}	64	36
DNA-SS-DNA (3)	6	6.9×10^{13}	72	28	2	1.8×10^{13}	61	39

MCH treatment on *short time* immobilized DNA					
Species	% S	Molecules/cm^2	% S_1	% S_2	Molecules incorporated on DNA SAM (%)[a]
MCH over (1)	17	2.0×10^{14}	77	23	51
MCH over (2)	20	2.4×10^{14}	75	25	77
MCH over (3)	22	2.6×10^{14}	80	20	74

[a] Ratio of surface density for each DNA type, before and after MCH treatment, calculated by use of Eq 2

alkanethiols system. This could be supported by the large differences between the adsorption modes of both DNA disulfides found by all the methods used in this study. Self-assembly depends highly on the characteristics of the molecule coupled to the disulfide bridge. In our study, having a long charged molecule coupled to the disulfide bridge (–SS–DNA) in contrast with a short organic uncharged one (-SS-DMTO) seems to play a key role in the ability of the DNA to chemisorb and to create dense monolayers. This is probably caused by the higher steric hindrance when having two identical DNA chains in a very close position. We suggest that it would favour the occurrence of repulsive forces between chains. This would result in a greater tendency of DNA chains to separate from each other, leading to the formation of large nucleotide–gold adsorptive contacts that contribute to less compacted monolayers, and probably to the occurrence of desorption phenomena. However, if the DNA chains at both sides of the disulfide bridge are complementary, repulsion between them does not occur and they self-assemble densely (Wackerbarth et al. 2004), demonstrating that this might be a critical factor in the chemisorption mechanism of disulfides.

Evaluation of DNA chemisorption efficiency using MCH

The efficiency of chemisorption of the three DNA types was analysed in parallel by measuring the fraction of MCH molecules able to immobilize in a preformed DNA SAM. This reflects the number of empty places in the DNA monolayer (the larger is this number, the lower is the ability of the pre-immobilized DNA to chemisorb). This evaluation was done for each DNA type using both nanomecanical and SPR biosensors (Fig. 2). The SPR signals (in refractive index change) for MCH immobilization were $5.4 \pm 2.1 \times 10^{-4}$, $6.6 \pm 3.9 \times 10^{-4}$, and $7.6 \pm 1{,}6 \times 10^{-4}$ for DNA-SH, DNA-SS-DMTO, and DNA-SS-DNA SAMs, respectively. As this sensor is sensitive to mass changes, large changes of refractive index values are representative of large amounts of MCH immobilized at the monolayer. On the other hand, the mean values of the MCH-induced surface stress in the nanomechanical biosensor at the DNA-SH, DNA-SS-DMTO, and DNA-SS-DNA monolayers were 120 ± 40, 140 ± 60, and 260 ± 140 mN/m, respectively. The nanomechanical values were used to normalize the cantilever deflection signal, enabling the analysis of the MCH contribution to the total surface stress signal. This was calculated as the ratio of the surface stress signal due to MCH to the total signal due to DNA plus MCH (Eq. 1):

$$\%\,\mathrm{MCH}_{\text{surface stress contribution}} = \frac{\sigma_{\mathrm{MCH}}}{\sigma_{\mathrm{DNA}} + \sigma_{\mathrm{MCH}}} \times 100 \qquad (1)$$

MCH contributions were 36, 56, and 73% for SH-DNA, DNA-SS-DMTO, and DNA-SS-DNA monolayers, respectively, evidence of the large differences between the behaviour of thiol and disulfide-modified DNA monolayers, especially for the DNA-SS-DNA monolayer.

As shown in Fig. 2, both biosensors registered a similar trend with a larger signal due to MCH at the DNA-SS-DNA monolayer, followed by smaller signals for the DNA-SS-DMTO and DNA-SH cases, as expected from the results of the DNA immobilization study. The signal of the MCH adsorption over a clean gold surface is also included for comparison; this is much larger than when adsorption was carried out upon a previously immobilized DNA SAM.

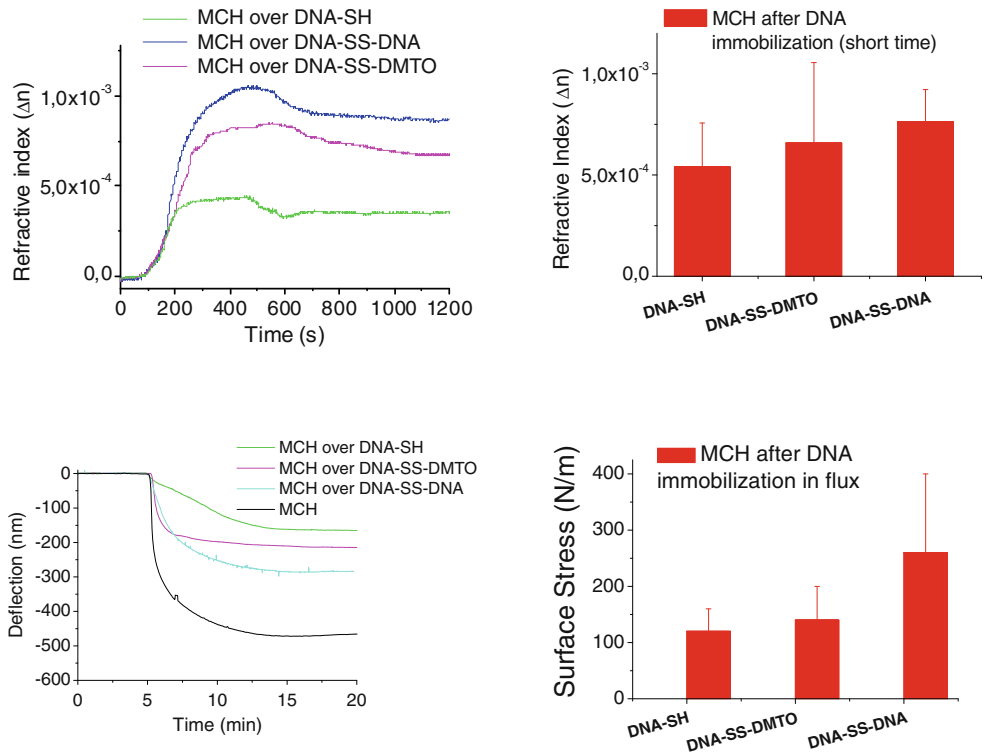

Fig. 2 MCH signals obtained by SPR (*top*) and nanomechanical biosensors (*bottom*) for each DNA monolayer type. *Right side*: statistics of mean values achieved for MCH treatment on each monolayer type

Figure 3 shows that after MCH adsorption almost full coverage of empty DNA vacant sites was reached. Neither unmodified DNA nor DNA-SH were able to be further adsorbed at the cantilever surface as the unmodified DNA did not give any deflection signal and the DNA-SH only gave a very small one of 25 nm.

XPS experiments also showed a high degree of MCH occupation for the three DNA monolayer types. After MCH immobilization, full coverage of the gold surface in the range of 2–2.6 $\times$ 10^{14} molecules/cm^2 was obtained in the three cases. The degree of occupation for each monolayer type was calculated from these data in a similar way to the nanomechanical case, as a relationship between MCH surface density and that of DNA before this treatment (Eq. 2).

$$\%\text{MCH Ocupation} = \left(\frac{\text{Surface density after MCH} - \text{DNA Surface density}}{\text{Surface density after MCH}}\right) \times 100 \quad (2)$$

The DNA-SH, DNA-SS-DMTO, and DNA-SS-DNA monolayers showed MCH occupation values of 51, 77, and 74%, respectively (Fig. 2), which strongly supports the evidence of greater ability of DNA-SH molecules to chemisorb, creating more densely packed monolayers in comparison with the DNA-disulfide molecules.

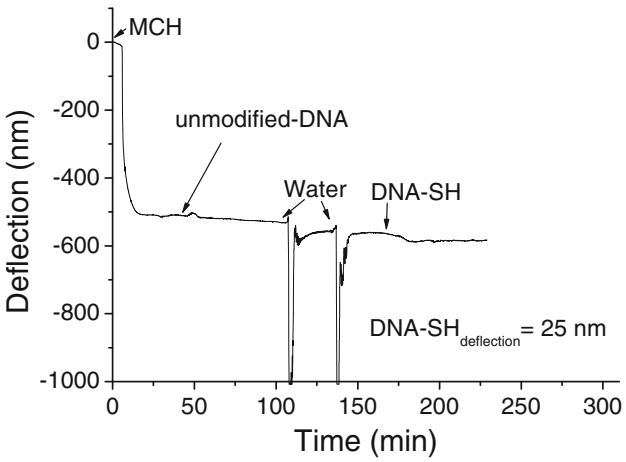

Fig. 3 MCH immobilization signal on nanomechanical biosensor, and subsequent injection of unmodified DNA and DNA-SH. It is shown that after MCH adsorption the unmodified DNA is unable to give any deflection signal. DNA-SH gives a very small signal of 25 nm only

The results indicated that DNA disulfide SAMs have a monolayer configuration with a large number of available places for MCH immobilization, which is supported by their lower surface densities and high physisorption degree with a laying down configuration of DNA probes. MCH adsorption could be accomplished by a mechanism of displacement of nucleotide–gold contacts, which leaves

empty places within the monolayer. The possibility of a thiol–thiol exchange mechanism has also been proposed (Steel et al. 2000). This means that the sulfur–gold bond between the DNA linked probe and the substrate could be exchanged for one between MCH and the substrate. According to Steel et al. (2000), probe desorption during MCH treatment is a result of thiol–thiol exchange for short probes, up to 24 b; it is, however, unclear whether the thiol–thiol exchange contribution could take place with the same extension for DNA thiols and disulfides. It is reasonable to expect that DNA monolayers that display lower surface densities with a high number of nucleotide–gold contacts could also be more susceptible to thiol–thiol exchange, which would be the case of DNA disulfides. Initially, the vacant surface sites around each probe leave available places once the nucleotide–gold contacts are removed; incoming MCH molecules can attack and displace a thiol–gold bond between a probe and the substrate. The larger signals found for MCH immobilization in the disulfide monolayers could therefore be explained by their lower surface densities, which leave a higher number of vacant places giving more opportunities to MCH for thiol exchange.

Analysis of DNA organization and spatial configuration during self-assembly and MCH treatment

The orientation of DNA molecules with regard to the gold surface was studied using fluorescence by taking into account the gold quenching effect on the DNA-tethered dye. The quenching effect induced by gold follows a $1/d^5$ tendency (Chance et al. 1978), which means that small changes in orientation, even of only 1 nm, can induce large changes in the fluorescent signal. For this reason, fluorescence is extremely useful for study of spatial distribution after DNA self-assembly (i.e. DNA molecules lying down over the surface or vertically positioned) (Stoermer and Keating 2006; Rant et al. 2004a, b; Arinaga et al. 2006; Lee et al. 2006).

For analysis of the fluorescent images, the ssDNA can be modelled as a discrete persistent chain whose ground state is in a zigzag configuration (Tkachenko 2007). With regard to the spatial conformations that DNA molecules can adopt during self-assembly, the literature indicates that highly dense monolayers tend to achieve a configuration with DNA chains aligned vertically and slightly tilted toward a $\sim 45^\circ$ angle with regard to the surface (Kelly et al. 1998), whereas poorly assembled monolayers favour a more horizontal configuration (Herne and Tarlov 1997; Rant et al. 2004), with molecules lying down over the surface.

Figure 4a shows the collected fluorescent signals for the DNA probes immobilized overnight. It can be observed that the highest fluorescent signal was achieved by the DNA-SH monolayer, followed by the DNA-SS-DMTO and the DNA-SS-DNA forms, respectively, whereas the non-thiolated DNA form produced an almost negligible fluorescence signal. As the unmodified form is only attached by physisorption, this molecule was probably adopting a complete lying-down conformation, suffering a large quenching effect. On the other hand, the DNA-SH monolayer, which displayed the largest fluorescence signal, must have a large surface density in a preferred upright configuration. As radiolabelling experiments showed similar surface coverages for the unmodified and DNA-SH monolayers, the different fluorescence between them can mainly be justified by the probe orientation with respect to the surface.

A large fluorescent signal was also obtained from DNA-SS-DMTO, which indicates an upright conformation similar to that of DNA-SH. In contrast, a much smaller signal was obtained from DNA-SS-DNA, which can be explained by a mixture of chemisorbed and physisorbed probes, although its low fluorescence suggest a large amount of probes lying down over the surface. These results were in agreement with those obtained with the nanomechanical biosensor and XPS.

Finally, in order to obtain deeper information, MCH treatment was performed on the three DNA monolayers. As the only labelled molecules are the DNA ones, the experiments enabled following of the removal of previously adsorbed probes and their configuration changes because of the presence of MCH within the monolayer. When the DNA monolayers were treated with MCH, the non-perfectly bound molecules and the thiol-exchanged ones are removed, as demonstrated by radiolabelling measurements in Fig. 1c. Removal of molecules produces a decrease of the fluorescence signal; however, because of the quenching effect, this fluorescence decrease might be counterbalanced by the increase of perfectly attached molecules that further increases the total fluorescent signal. Both effects are presented in the images shown in Fig. 4a. For DNA-SH and DNA-SS-DMTO, a decrease of the initial fluorescence is measured, whereas for DNA-SS-DNA the opposite trend is observed. An explanation could be that the removal of probes by the MCH took place for all DNA types, although much more intensely for disulfides. Therefore, the fluorescent signal was substantially reduced on the disulfides with regard to the DNA-SH. As the DNA-SH monolayer has a large surface density, the molecules might be closely positioned and slightly tilted toward a 45° angle in a dense monolayer. For less densely packed monolayers, molecules might be more vertically positioned, because of the raising up effect of MCH. The more the MCH is incorporated, the more upright are the DNA probes. In the DNA-SH, the large surface density counterbalanced the larger quenching

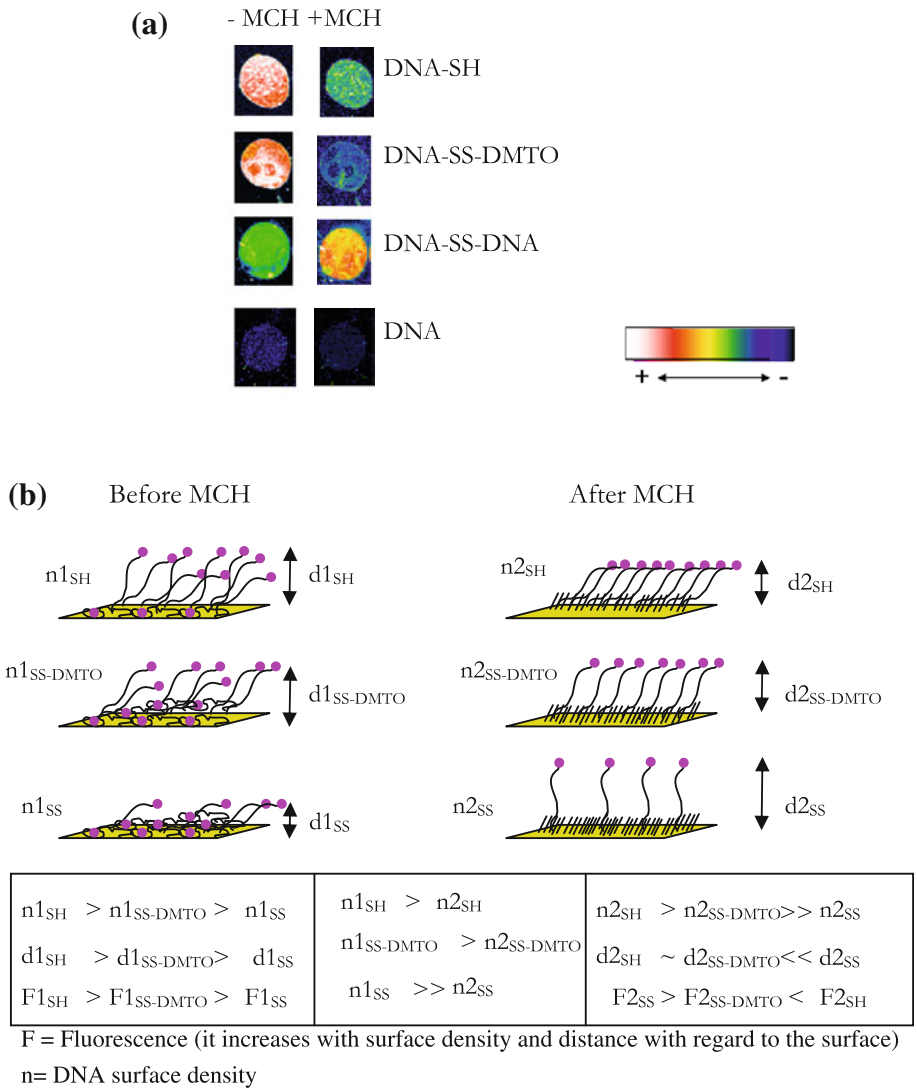

Fig. 4 **a** Fluorescence signals for the immobilisation of DNA-SH, DNA-SS-DMTO, and DNA-SS-DNA SAMs and the effect of a post-MCH treatment on the global fluorescence. Images are given in an artificial colour scale in which *white* is the colour assigned to the largest amount of fluorescence-labelled molecules whereas *black* is assigned to the absence of fluorescent molecules. **b** Model of DNA adsorption for each sulfur linker type according to fluorescence experiments and to the results obtained by biosensors and XPS methods

because of the tilted position of the molecules, giving large fluorescence. For the DNA-DMTO there was still a large surface density, but lower than for the DNA-SH. The molecules would be more vertically oriented, but a smaller number of fluorescent probes compared with the DNA-SH would explain its lower fluorescence. For the DNA-SS-DNA, having the lowest surface density would lead to molecules even more vertically oriented, which, besides the smaller number of fluorescent probes, would lead to a larger fluorescence signal than for the other two cases.

Arianaga et al. (2006) followed the effect of MCH adsorption in a DNA-SH monolayer by use of fluorescence. They also observed substantial removal of DNA probes shortly after MCH treatment of highly dense monolayers, as was observed for DNA-SH and DNA-SS-DMTO in our experiments. Later MCH treatments did not cause further DNA desorption. They demonstrated the mechanism mediating DNA conformation change due to MCH adsorption. MCH causes a drop in the surface potential of gold electrodes which is characteristic for an oxidative adsorption process. This means injection of electrons into the substrate on formation of the S–Au bond, which causes a change in the surface charge. The change in the surface charge would be responsible for removing the nucleotide–gold contacts inducing a change in DNA orientation from lying down to upright. This suggests that the conformation of DNA strands is predominantly governed by electric interactions with the (charged) substrate that supports the layer as a consequence of the presence of MCH within the monolayer. This explanation would help to explain the DNA-SS-DNA case. For this molecule its low surface density and the high degree of MCH adsorption on the monolayer would lead to introduction of a large surface charge change responsible of a greater upright configuration than for the other two cases.

Additionally, a second quenching mechanism might be responsible for the differences between DNA-SS-DNA and the other two DNA types after MCH adsorption. It is

known that fluorescent dyes can undergo lateral non-radiative energy transfer (self-quenching) when they are in a much closer position (Lakowicz 1999). It is possible that dyes of the DNA-SH and DNA-SS-DMTO probes could be partially self-quenched in comparison with the DNA-SS-DNA case, where the higher degree of MCH incorporation would lead to greater distance between neighbouring dyes and reduction of the self-quenching effect.

Arianaga et al. (2006) also noticed the formation of holes caused by further DNA desorption when MCH-treated samples were stored in buffer overnight. In these samples, MCH causes the release of DNA probes and their reorganization within the monolayer. In our experiments, as we evaluated the MCH-treated samples immediately after their formation without previous storage, this later desorption–reorganization process should not be taking place and was not observed in our experiments.

On the basis of the above results, we propose the following model in order to explain the behaviour and spatial organization of each DNA monolayer (Fig. 4b):

- Initially all DNA molecules show large immobilization, but the final surface density displays the following trend DNA-SH > DNA-SS-DMTO > DNA-SS-DNA. As a result, DNA-SH and DNA-SS-DMTO molecules are more vertically positioned, exhibiting a higher fluorescence signal than the DNA-SS-DNA case where molecules are mostly lying down on the surface, suffering a high quenching effect.
- After MCH treatment, strong replacement of the DNA molecules induces a surface density decrease that lowers the fluorescence signal. At the same time, MCH incorporation induces a change in the surface charge that raises the lying-down probes. This effect is observed in all DNA SAMs types; its extent is in the sequence DNA-SS-DNA $\gg$ DNA-SS-DMTO $\geq$ DNA-SH. The more the MCH is incorporated into the monolayer, the more the DNA molecules are vertically positioned, with a lower quenching effect.
- A self-quenching effect between neighbouring DNA probes that could contribute to reducing the DNA-SH and DNA-SS-DMTO fluorescence signals must be also taken into account.

Conclusions

Experiments performed by nanomechanical and surface plasmon resonance biosensors and by use of the ex-situ techniques, fluorescence measurement and radiolabelling, have highlighted the critical role of the form of the sulfur linker in the self-assembly of DNA receptor molecules. The results obtained using nanomechanics are of special interest because this method has the ability to distinguish between chemisorbed and physisorbed states and also revealed that the surface stress signal is especially affected by the chemisorption itself, rather than for the quantity of immobilized probes.

Our experiments furnished clear evidence that the SH linker form has greater ability to chemisorb than the disulfide forms. The disulfide forms showed greater physisorption phenomena and desorption at long immobilization times. These values were particularly pronounced in the dimeric form of DNA, the DNA-SS-DNA, which was the most handicapped toward immobilization. In addition, differences in DNA configuration and spatial distribution during self-assembly and MCH treatment have been found to be a consequence of the sulfur-modification type.

MCH has also been used to confirm immobilization data and to reveal the efficiency of each sulfur linker to create dense self-assembled monolayers. Results obtained after MCH treatment showed higher occupation of MCH molecules in DNA SAMs derivatized with disulfide linker forms, also supporting the lower efficiency of these molecules to self-assembly. This is evidence of the need to use DNA probes in the SH form and the need to perform immobilization procedures that avoid the formation of disulfides, to produce monolayers of excellent quality for biosensing.

Our results are likely to be of interest for DNA detection methods based on biosensors which are strongly affected by the efficiency of assembly of DNA receptors on a solid surface, in order to enhance the DNA detection.

Acknowledgments L.M., Y.H., and E.R. acknowledge the Nanoselect Project (CSD2007-00041) from the Spanish Ministry for Innovation and Science. L.G.C. and L.M.L. acknowledge funding from Fundation Botin.

References

Alvarez M, Carrascosa LG, Moreno M, Calle A, Zaballos A, Lechuga LM, Martinez-A C, Tamayo J (2004) Nanomechanics on the formation of DNA self-assembled monolayers and hybridisation on microcantilevers. Langmuir 20(22):9663–9676

Arinaga K, Rant U, Tornow M, Fujita S, Abstreiter G, Yokoyama N (2006) The role of surface charging during the coadsorption of mercaptohexanol to DNA layers on gold: direct observation of desorption and layer reorientation. Langmuir 22:5560–5562

Bain CD, Biebuyck HA, Whitesides GM (1989) Comparison of self-assembled monolayers on gold: coadsorption of thiols and disulfides. Langmuir 5:723–727

Biebuyck HA, Bain CD, Whitesides GM (1994) Comparison of organic monolayers on polycrystalline gold spontaneously assembled from solutions containing dialkyl disulfides or alkanethiols. Langmuir 10:1825–1831

Cavalleri O, Oliveri L, Daccà A, Parodi R, Rolandi R (2001) XPS measurements on Image -cysteine and 1-octadecanethiol self-assembled films: a comparative study. Appl Surf Sci 175–176:357–362

Cavalleri O, Gonella G, Terreni S, Vignolo M, Pelori P, Floreano L, Morgante A, Canepa M, Rolandi R (2004) High resolution XPS of the S 2p core level region of the L-cysteine/gold interface. J Phys: Condens Matter 16:S2477–S2482

Chance R, Prock A, Silbey R (1978) Molecular fluorescence and energy transfer near interfaces. Adv Chem Phys 37:1

Fenter P, Eberhardt A, Eisenberger P (1994) Self-assembly of n-alkyl thiols as disulfides on Au(111). Science 266:1216

Garg N, Friedman J, Lee T (2000) Adsorption profiles of chelating aromatic dithiols and disulfides: comparison to those of normal alkanethiols and disulfides. Langmuir 16:4266–4271

Herne T, Tarlov MJ (1997) Characterization of DNA probes immobilized on gold surfaces. J Am Chem Soc 119:8916–8920

Homola J (2008) Surface plasmon resonance sensors for detection of chemical and biological species. Chem Rev 108(2):462–493

Huang H-M, Chang C-Y, Liu I-C, Tsai H-C, Lai M-K, Tsiang RC-C (2005) Synthesis of gold nanocomposite via chemisorption of gold nanoparticles with poly(p-methyl styrene) containing multiple bonding groups on the chain side. J Polym Sci: Part A: Polym Chem 43:4710–4720

Jung C, Dannenberger O, Xu Y, Buck M, Grunze M (1998) Self-assembled monolayers from organosulfur compounds: a comparison between sulfides, disulfides and thiols. Langmuir 14:1103

Kelly S, Barton J, Jackson N, McPearson L, Potter A, Spain E (1998) Orienting DNA helices on gold using applied electric fields. Langmuir 14:6781–6784

Lakowicz J (1999) In principles of fluorescence spectroscopy. Kluwer Academic/Plenum, New York, pp 237–265

Lee C-Y, Gong P, Harbers GM, Grainger DW, Castner DG, Gamble LJ (2006) Surface coverage and structure of mixed DNA/alkylthiol monolayers on gold: characterization by XPS, NEXAFS, and fluorescence intensity measurements. Anal Chem 78(10):3326–3334

Martínez L, Carrascosa LG, Huttel Y, Lechuga LM, Roman E (2010) Influence of the linker type on the Au-S binding properties of thiol and disulfide-modified DNA self-assembly on polycrystalline gold. Phys Chem Chem Phys 12(13):3301–3308 (doi: 10.1039/b924504a)

Mauriz E, Calle A, Abad A, Montoya A, Hildebrandt A, Barcelo D, Lechuga LM (2006) Determination of carbaryl in natural water samples by a surface plasmon resonance flow-through immunosensor. Biosens Bioelectron 21(11):2129–2136

Moulin AJ, O'Shea SJ, Welland ME (2000) Cantilever-based biosensors. Ultramicroscopy 82:23–31

Munro JC, Frank CW (2003) Adsorption of disulfide-modified polyacrylamides to gold and silver surfaces as cushions for polymer-supported lipid bilayers. Polymer 44:6335–6344

Noh J, Hara M (2001) Nanoscale observation of dissociative adsorption during self-assembly processes of dialkyl disulfides on Au(111). Rinken Review 37:54–57

Noh J, Murase T, Nakajima K, Lee H, Hara M (2000) Nanoscopic investigation of the self-assembly processes of dialkyl disulfides and dialkyl sulfides on Au(111). J Phys Chem B 104:7411–7416

Rant U, Arinaga K, Fujita S, Yokoyama N, Abstreiter G, Tornow M (2004a) Structural properties of oligonucleotide monolayers on gold surfaces probed by fluorescence investigations. Langmuir 20(23):10086–10092

Rant U, Arinaga K, Fujita S, Yokoyama N, Abstreiter G, Tornow M (2004b) Dynamic electrical switching of DNA Layers on a metal surface. Nano Letters 4(12):2441–2445

Sako EO, Kondoh H, Nakai I, Nambu A, Nakamura T, Ohta T (2005) Reactive adsorption of thiophene on Au(111) from solution. Chem Phys Lett 413:267–271

Steel AB, Levicky RL, Herne TM, Tarlov MJ (2000) Immobilization of nucleic acids at solid surfaces: effect of oligonucleotide length on layer assembly. Biophys J 79:975–981

Stoermer R, Keating C (2006) Distance-dependent emission from dye-labeled oligonucleotides on striped Au/Ag nanowires: effect of secondary structure and hybridization efficiency. J Am Chem Soc 128(40):13243–13254

Tkachenko AV (2007) Elasticity of strongly stretched ssDNA. Physica A 384:133–136

Wackerbarth H, Marie R, Grubb M, Zhang J, Hansen AG, Chorkendorff I, Christensen CBV, Boisen A, Ulstrup J (2004) Thiol- and disulfide-modified oligonucleotide monolayer structures on polycrystalline and single-crystal Au(111) surfaces. J Solid State Electrochem 8:474–481

Willey TM, Vance AL, Buuren TV, Bostedt C, Terminello LJ, Fadley CS (2005) Rapid degradation of alkanethiol-based self-assembled monolayers on gold in ambient laboratory conditions. Surf Sci 576:188–196

Wirde M, Gelius U, Dunbar T, Allara DL (1997) Modification of self-assembled monolayers of alkanethiols on gold by ionizing radiation. Nucl Instr Meth Phys Res B 131(1):245–251

Wolf LK, Gao Y, Georgiadis RM (2004) Sequence-dependent DNA Immobilization: specific versus nonspecific contributions. Langmuir 20:3357–3361

Zerulla D, Uhlig I, Szargan R, Chasse T (1998) Competing interaction of different thiol species on gold surfaces. Surf Sci 402–404:604–608

Zhang H-L, Evans SD, Critchley K, Fukushima H, Tamaki T, Fournier F, Zheng W, Carrez S, Dubost H, Bourguignon B (2005) Novel cyanoterphenyl self-assembly monolayers on Au(111) studied by ellipsometry, X-ray photoelectron spectroscopy, and vibrational spectroscopies. J Chem Phys 122:224707